THE POTENTIAL FOR GLACIAL FLOUR TO ACT AS ICE NUCLEI IN CLOUDS

A dissertation submitted to the University of Manchester
for the degree of Master of Science
in the Faculty of Science and Engineering

2017

Victoria L. Trost
School of Earth and Environmental Sciences

Contents

Word count 6970

List of Tables

List of Figures

Abstract

The influence of mineral and dust particles on the immersion freezing mode of ice nucleation has been an area of active research. Most studies focus on dusts from tropical to mid-latitude regions with high latitude dusts remaining mostly unexplored. The goal of this study was to provide an initial evaluation on the ice nucleation efficiency of glacial flour, a natural dust that is common in many high latitude dust source regions. The glacial flour sample used in this study originated from the Findelen Glacier in Switzerland. Surface area and mineral composition analyses were performed and a cold-stage freezer method was used to determine the immersion freezing temperatures of water drops containing glacial flour particles. NX-illite, illite, and kaolinite samples were also tested to verify that the experiment method produced results consistent with previous studies and to be a same-method comparison for the glacial flour. The ice nucleation efficiency of the samples was quantified by using a deterministic approximation to calculate the ice-active surface site density from the freezing temperature and particle surface area data. The glacial flour showed a similar ice nucleation efficiency to NX-illite with a freezing temperature range between $-9.6\,^{\circ}\mathrm{C}$ and $-21.6\,^{\circ}\mathrm{C}$ and $n_s(T)$ range between 3.0×10^{-3} cm^{-2} and 4.1×10^{0} cm^{-2}. These results suggest that the glacial flour sample does not have a particularly high ice nucleation efficiency, but rather falls around mid-range of the pure minerals and natural dusts that have been studied previously. Ranking the importance of the constituents of the glacial flour sample based on both weight percent and surface area percent suggests that the latter may be a better representative of ice nucleation efficiency. Pre-activation could also have an impact on the ice nucleation efficiency of glacial flour, but is only discussed qualitatively here.

Declaration

No portion of the work referred to in the dissertation has been submitted in support of an application for another degree or qualification of this or any other university or other institute of learning.

Intellectual Property Statement

i. The author of this dissertation (including any appendices and/or schedules to this dissertation) owns certain copyright or related rights in it (the "Copyright") and s/he has given The University of Manchester certain rights to use such Copyright, including for administrative purposes.

ii. Copies of this dissertation, either in full or in extracts and whether in hard or electronic copy, may be made **only** in accordance with the Copyright, Designs and Patents Act 1988 (as amended) and regulations issued under it or, where appropriate, in accordance with licensing agreements which the University has entered into. This page must form part of any such copies made.

iii. The ownership of certain Copyright, patents, designs, trade marks and other intellectual property (the "Intellectual Property") and any reproductions of copyright works in the dissertation, for example graphs and tables ("Reproductions"), which may be described in this dissertation, may not be owned by the author and may be owned by third parties. Such Intellectual Property and Reproductions cannot and must not be made available for use without the prior written permission of the owner(s) of the relevant Intellectual Property and/or Reproductions.

iv. Further information on the conditions under which disclosure, publication and commercialisation of this dissertation, the Copyright and any Intellectual Property and/or Reproductions described in it may take place is available in the University IP Policy (see http://documents.manchester.ac.uk/DocuInfo.aspx?DocID=487), in any relevant Dissertation restriction declarations deposited in the University Library,

The University Library's regulations (see http://www.manchester.ac.uk/library/aboutus/regulations) and in The University's Guidance on Presentation of Dissertations.

Acknowledgements

Thank you to my supervisors, Paul Connolly and David Schultz, for their guidance and support. Also to Steve Boult who provided the glacial flour sample and John Waters who performed the XDR and BET analyses.

Chapter 1

Introduction

Understanding ice nucleation is key to understanding cloud and precipitation properties. The interplay of air temperature, moisture content, and aerosol concentration and properties determines how water in the atmosphere changes between phases and, in turn, how clouds and precipitation behave. Pure water drops can remain in an unfrozen, supercooled state down to $-40\,^{\circ}\mathrm{C}$ at which point the drops will freeze spontaneously (Rogers and Yau, 1996); this is known as homogeneous freezing. Homogeneous deposition of ice, which is the process of pure ice forming directly from vapor, is theoretically possible, but is not observed in the atmosphere due to the extremely high supersaturation required (Vali et al., 2015). Ice is regularly found in environments that are warmer than the range for homogeneous nucleation; this is due to the influence of aerosol particles. Aerosol particles enhance ice nucleation by lowering the energy barrier required for a phase transition to occur. This means that heterogeneous nucleation can occur at lower supersaturations and supercoolings than is required for homogeneous nucleation.

There are four potential heterogeneous ice nucleation methods: deposition nucleation, immersion freezing, condensation freezing, and contact freezing. Deposition nucleation is the process in which ice forms on a particle directly from the vapor phase. Immersion freezing is the process in which a particle immersed inside a liquid drop triggers ice formation. In condensation freezing, vapor first condenses onto a particle and then that liquid freezes. Contact freezing occurs when a supercooled drop collides

with a particle and the contact triggers freezing. Immersion freezing is considered to be the dominant method in mixed-phase clouds (Augustin-Bauditz et al., 2014; Tobo, 2016), and so will be the focus of this paper.

Immersion freezing is only possible in environments containing aerosol particles. Total aerosol concentrations in the atmosphere tend to range from around 10^2 to 10^4 cm^{-3}. The concentration of aerosols that can act as an ice nucleating particle (INP) is lower at only around 10^{-4} to 10^{-1} cm^{-3} (Murray et al., 2012). There are a variety of aerosols that can be found in the atmosphere, but one of the most important for ice nucleation is mineral dust. Estimates of global mineral dust aerosol emissions range from 1000 to 3000 Tg per year (Thorsteinsson et al., 2011; Murray et al., 2012). The primary dust source regions are arid, tropical to mid-latitude regions. Prospero et al. (2002) defines a "global dust belt" that extends eastward from North Africa to China and covers the dominate dust sources. These arid regions are the focus of most dust emission studies because of their emission strength, but higher latitude dust sources can have a substantial impact as well, particularly in areas near the source regions.

One form of high latitude dust is glacial flour. Glacial flour is also formed by mid-latitude glaciers, but its importance as an INP is expected to be greater at higher latitudes where other aerosol sources are weaker. Glacial flour is a fine-grained mineral dust that is formed by erosion of the bedrock and sediment under glaciers and is carried away from the glaciers in glacial outwash and floods. The dust is then deposited on flood plains and riverbeds where it can become airborne after drying. The emission of such dust deposits depends on wind speed, snow cover, and vegetation, which leads to a strong seasonal variation in dust emission amounts. For example, in Iceland the peak period for dust storms is in late spring to early summer after early spring floods renew the dust deposits. In contrast, Alaska has a peak emission period in the autumn due to snow cover lasting until early summer (Prospero et al., 2012; Groot Zwaaftink et al., 2017). Climate change also influences variations in the emission amounts. Thorsteinsson et al. (2011), Prospero et al. (2012), and Bullard et al. (2016) agree that glacial dust emissions will increase as glaciers retreat because that process will expand dust deposits.

Glacial flour is defined by the physical weathering of subglacial material, because of this, the mineral composition of glacial flour varies depending on the source region. In regions with a history of volcanic activity, such as Iceland, Alaska, and Oregon, glacial flour can be composed of mostly volcanic material. For example, glacial flour samples collected from the proglacial valleys of the Collier and Diller Glaciers in Oregon were found to contain mostly plagioclase and pyroxene, which are two of the minerals that make up basalt, a form of volcanic rock (Rampe et al., 2017). Similarly, Dagsson-Waldhauserova et al. (2014) analyzed dust from near the Myrdalsjokull Glacier in Iceland and found that its composition was dominated by volcanic glass, plagioclase, and pyroxene. In contrast, glacial flour from locations such as the Monte Rosa massif in the Pennine Alps, would be primarily quartz and feldspars due to the bedrock being mostly granitoids (Froitzheim, 2001).

Understanding the bulk composition of a sample is a first step in understanding its ice nucleation efficiency. Further information beyond the bulk composition is needed because the ice nucleation efficiency of a sample is not determined by the bulk composition alone, but rather on the characteristics of discrete nucleation sites on the particle surface. This is one of the reasons why different studies can produce different results for the same mineral. For example, Zolles et al. (2015) tested three different quartz samples and found that the median freezing temperature of the samples covered a range of 14 °C despite all the samples containing the same mineral. This range in ice nucleation efficiency was attributed to differences in the density of nucleation sites on the particles in each sample.

The ice nucleation efficiency of a particle depends on the physical and chemical characteristics of the nucleation sites. Surface defects, such as atomic lattice distortions and crystallographic dislocations, can cause a local enhancement of ice nucleation if the size and structure are a good match to the structure of ice. In this situation, the defects act as a guide or template to help water molecules become arranged into an ice-like structure. The impact of hydrogen bond strength between water molecules and surface ions can vary depending on the ions and surface structure being considered. Strong hydrogen bonds can enhance ice nucleation if they bond water molecules to a

structure that is a good match for ice, but inhibit ice nucleation if there is a structure mismatch. An ion can be classified as either a chaotrope or kosmotrope depending on its ability to either enhance or inhibit the structure of water (Marcus, 2009; Zolles et al., 2015). Chaotropes interact strongly with water molecules and as a result inhibit the ability of the water molecules to form an ice-like structure in the presence of the ions. Kosmotropes bond more weakly with water, and so do not inhibit water structure formation like chaotropes do. The size of the ions can also have an impact on the ability for an ice-like structure to be formed. Similar to the surface structure matching impacts, the size of an ion can either enhance ice formation, if it fits well into the ice structure, or inhibit ice formation, if its size disrupts the structure. These ion impacts are thought to cause the differences in ice nucleation efficiency between different types of feldspar (Zolles et al., 2015). While it is not generally feasible to determine the ice nucleation efficiency of the individual nucleation sites, recognizing the existence and import of such sites is needed to accurately interpreting ice nucleation efficiency data.

A common way to quantify the impact of the nucleation sites is to determine the ice nucleation efficiency of a material by calculating the material's ice-active surface site density (IASSD). This method is based on the assumption that nucleation occurs at discrete sites on the surface of the particle and that nucleation at these sites occurs at a specific temperature. As such, this method is a singular or deterministic approximation. By classic nucleation theory, ice nucleation is a stochastic process and has a time-dependence as well as a temperature-dependence. However, studies have shown that in general the time-dependence is of small importance compared to temperature and INP dependences, and so can be considered negligible leading to the singular approximation used here (e.g. Connolly et al., 2009; Broadley et al., 2012; Murray et al., 2012; Ervens and Feingold, 2013; Hiranuma et al., 2015).

The IASSD is the number of sites per surface area that have activated nucleation between 0 °C and temperature T, and is given by Eq. (1.1)

$$n_s(T) = \frac{-ln(1 - f_i(T))}{A} \tag{1.1}$$

where T is the temperature, $n_s(T)$ is the ice-active surface site density as a function of T, $f_i(T)$ is the fraction of drops frozen at T, and A is the total surface area of the

particles in the drop. The fraction frozen, $f_i(T)$, is given by Eq. (1.2)

$$f_i(T) = \frac{N_i(T)}{N} \tag{1.2}$$

where $N_i(T)$ is the number of drops frozen at T and N is the total number of frozen and unfrozen drops (Connolly et al., 2009).

There are multiple experimental methods available to determine the ice nucleation efficiency of particles, and they can be divided into two general categories: drops suspended in a gas and drops held on a surface. Methods using drops suspended in a gas, also known as chamber methods, include: cloud expansion chambers, continuous flow diffusion chambers, wind tunnels, laminar flow chambers, free falling droplet systems, electrodynamic levitation, and aerosol flow tubes. Methods where the drops are held on a surface, also known as cold-stage methods, involve depositing the drops either on a hydrophobic surface or within oil (Murray et al., 2012).

The goal of this study was to provide an initial evaluation on the potential ability of glacial flour to act as an INP in immersion freezing. The glacial flour sample tested represents a type of natural dust aerosol that has not previously been studied in regards to ice nucleation, but may be a dominant INP at high latitudes. A simple cold stage method was used, and tests were also performed using NX-illite, illite, and kaolinite so that the experiment results could be compared to literature values and to act as a same-method comparison for the glacial flour.

Chapter 2 describes the samples and experimental method used in this study. Some of the advantages and potential challenges of the method are also discussed. In chapter 3 the results of the study are presented and compared with results from literature. Chapter 4 presents an evaluation of the contribution of the glacial flour constituent minerals based on weight percent and surface area percent. The differences between glacial flour and desert dust are also discussed. An overview of dust emission strength of six source regions is provided. The chapter ends with a discussion of the potential impact of pre-activation. Lastly, chapter 5 concludes the paper.

Chapter 2

Materials and Method

2.1 Materials

In this study, four samples were evaluated. There were two pure mineral samples, illite and kaolinite respectively. One sample was NX-illite, which is a manufactured dust that is composed of mostly illite (around 70 to 90 wt%) and at most around 10 wt% each of other minerals such as quartz, kaolinite, calcite, and feldspar (Hiranuma et al., 2015). Lastly, one sample was glacial flour, which is a natural dust. Illite and kaolinite were studied to verify that the experimental method could produce results consistent with literature values. NX-illite was used alongside illite and kaolinite for comparison with literature values and was also used as a same-method comparison value for the glacial flour. These reference samples were chosen because they were readily available on hand and these substances had been evaluated in previous studies, allowing the results from this study to be compared to literature values. Glacial flour was the sample of interest because no such study had been performed on the dust before.

2.1.1 Reference Materials

Only the freezing temperatures were of interest for illite and kaolinite, so no further details of those powders were needed. For the NX-illite, the Brunauer-Emmett-Teller (BET) surface area was needed to calculate the $n_s(T)$ values. The BET surface area

was assumed to be the literature value of 104.2 m^2g^{-1} (Emersic et al., 2015; Whale et al., 2015). BET surface area was the chosen specific surface area method because it is the most commonly used method and it provides more accurate values than a size based calculation method that uses the assumption of perfect spherical particles.

2.1.2 Glacial Flour

Glacial flour is a fine-grained mineral dust which is the result of glacial erosion. The glacial flour used in this study was collected from an outwash of the Findelen Glacier near Zermatt, Switzerland. The Findelen Glacier is one of the many glaciers within the Monte Rosa massif. The mineral composition of the glacial flour was evaluated via X-ray powder diffraction (XDR) using the University of Manchester's Bruker D8Advance X-Ray Diffractometer. XDR is a rapid analytical technique for evaluating the composition of mineral and dust samples and is the most common technique used in literature. The composition of the sample is determined by bombarding the sample with X-rays and then recording the intensity of the diffracted X-ray beams over a range of angles. The plot of intensity as a function of angle, which is called a diffractogram, is then compared to the diffractorgrams of pure minerals in a standard reference database to identify the minerals present in the sample. The resulting diffractogram for the glacial flour sample is given in Figures A.1 and A.2 and the quantified composition is presented in Table 2.1. The BET surface area of the glacial flour particles was determined using the University of Manchester's Gemini 2360 Surface Area Analyser and was found to be 4.7160 ± 0.0345 m^2g^{-1}.

Table 2.1: Composition of glacial flour as determined by X-ray powder diffraction. Minerals are listed in descending order by weight percent. The wt% and Error % were generated using the Topas software, which uses a non-linear least squares fitting system. For more information see Brucker-AXS (2008) and the references there in.

Name	wt%	Error %
Quartz	70.246	3.919
Albite, ordered (Na Feldspar)	16.470	2.184
Muscovite 1M	4.617	4.006
Protomangano-ferro-anthophyllite	4.195	1.475
Clinochlore llb-2	3.708	1.556
Montmorillonite, heated, oriented	0.746	0.638

2.1.3 Sample Preparation

For each sample, suspensions were made using 50 mL of pure (Milli-Q) water. The three reference samples were already in powder form, and so no further sample preparation was needed before forming the suspensions. The glacial flour came in chunks that were milled into a fine powder using a mortar and pestle.

Some other studies of minerals and dusts use milling processes that produce particles of a specified size and use rigorous stirring methods that can take between a couple hours to a day or more. For this study basic hand milling and stirring were used. The reason for this is that the scope of this study was to provide an initial evaluation of the potential ice nucleation efficiency of the glacial flour sample, and so putting in the time and resources for more involved milling and stirring was deemed unnecessary.

The powders were weighed gravimetrically to form suspensions of the chosen weight percents. All the samples were tested using 1 wt% suspensions because this weight percent value is the most common reported in literature. Suspensions of 0.1 wt% were also tested for the glacial flour to get a sense of how concentration impacts the nucleation efficiency, and the particular value was chosen because it is another common

value in literature.

2.2 Experiment Method

To evaluate the ice nucleation efficiency of the samples, a cold-stage freezer method was used to determine the freezing temperatures of water drops containing immersed particles. Some advantages of using this type of method are that the equipment setup is simple and inexpensive and experiments can be run typically within thirty minutes from start to finish. Cold-stage methods also allow larger drop sizes to be studied than would be possible with chamber methods. Larger drops have the advantage of easier handling because they can be formed and deposited using a pipette and can be visually inspected without magnification. Larger drops also have the advantage that they can be used to detect rare, but potentially highly efficient, INP which chamber methods are unable to measure due to an inability to detect low INP numbers. This leads to cold-stage methods generally giving results at the lower end of the IASSD spectrum and higher freezing temperatures while chamber methods can reach lower temperatures and higher IASSD values (Murray et al., 2012; Hiranuma et al., 2015; Tobo, 2016).

2.2.1 Method Details

Drops of the suspensions were pipetted onto a glass microscope slide, which had been coated with Rainx Rain Repellent to form a hydrophobic surface. Each slide held fourteen drops of 15 μL volume. Drops of this size were used because of their ease of handling and they could be clearly observed without magnification. The slide was then placed on a steel disk that was 10 cm in diameter and 2 cm thick and attached to a Pico Technology thermocouple data logger. The disk was then placed on a stand inside a chest freezer and covered with a glass dish to reduce contamination of the drops from the ambient air inside the freezer. The temperature of the steel disk was measured at a collection rate of one measurement per second, and a video of the drops freezing was recorded using a webcamera. The cooling rate varied slightly between

runs but was on average around $-4\,^{\circ}\mathrm{C}$ per minute. After all the drops had frozen, the steel disk was removed from the freezer and allowed to defrost. To determine the freezing temperature of each drop, the video was visually inspected frame by frame to find the time-step at which each drop froze. The temperature at that time-step was then extracted from the temperature data. The data logger has a quoted accuracy of 0.2% of the reading and precision of $\pm 0.5\,^{\circ}\mathrm{C}$. The output values were rounded to the nearest tenth of a degree.

For each sample, one to six runs were performed. Each run consisted of three or more fourteen-drop trials drawn from a single suspension. See Table 2.2 for details on the trials tested. Performing a minimum of three trials per run was chosen to check repeatability and lessen the impact of outliers. The reason there were so many pure water runs is because the experimental method was still be tested and practiced. Two runs were performed with NX-illite to verify that the method would produce repeatable results. Four runs were performed using 1 wt% glacial flour suspensions because that concentration value was the main focus of this study. For the 0.1 wt% glacial flour suspension two runs were deemed sufficient to represent how decreasing the concentration impacts the $n_s(T)$ values.

Table 2.2: Overview of experimental runs performed. For each sample 1 to 6 runs were performed. Each run represents a single suspension and from that suspension 3 or more trials of fourteen drops each were taken. The exact weight percent of each suspension is also listed.

Run	Trials	wt%
Pure water - run 1	10	
Pure water - run 2	5	
Kaolinite - run 1	3	0.98
Illite - run 1	4	0.98
NX-illite - run 1	4	1.1
NX-illite - run 2	3	1.1
Glacial flour 1 - run 1	3	1.1
Glacial flour 1 - run 2	3	1.1
Glacial flour 1 - run 3	3	1.0
Glacial flour 1 - run 4	3	1.1
Glacial flour 0.1 - run 1	3	0.11
Glacial flour 0.1 - run 2	3	0.11

2.2.2 Method Artifacts

Whenever data collection methods are being used there is the potential of unnatural results being produced due to the influences or limitations of the equipment. These unnatural results are often called artifacts and need to be dealt with by making changes to the collection method, applying corrections to the produced data, or a combination of the two. Artifacts that can occur in cold stage methods have been identified by previous studies (e.g. Hiranuma et al., 2015; Whale et al., 2015; Tobo, 2016). The primary artifact that was identified in this study was the impact of the ambient freezer air on the drop freezing temperature. Initial tests with pure water were performed without covering the stage and resulted in drops freezing as high as $-7.7\,^{\circ}\mathrm{C}$ and with a mean freezing temperature of $-18.7\,^{\circ}\mathrm{C}$. This was most likely caused by ice crystals and particles within the ambient air in the freezer coming into contact with the drops and initiating nucleation. By placing a glass dish over the stage the impact of the

ambient air was reduced resulting in an initial freezing temperature of −13.3 °C and a mean freezing temperature of −21.4 °C for the pure water. While these values are higher than the −40 °C freezing temperature that can be reached in supercooled water (Rogers and Yau, 1996), this discrepancy is expected because relatively large drops were used.

One of the biggest challenges faced when using larger drops is that the likelihood of contamination within the drops or at the interface between the drops and the substrate is relatively high. This contamination issue means that most cold-stage setups are unable to get drops down to the lowest temperatures because even drops without any immersed particles will freeze before the expected homogeneous freezing temperature (Murray et al., 2012; Hiranuma et al., 2015; Whale et al., 2015). However, with careful control of the experiment environment this contamination impact can be reduced or removed (Tobo, 2016).

Drop size alone can also lead to higher freezing temperatures because the freezing temperature of a drop is proportional to drop size (Whale et al., 2015; O and Wood, 2016; Tobo, 2016). Using classical nucleation theory, O and Wood (2016) derived an approximation for the homogeneous freezing temperature of water as a function of drop volume and water activity, which agreed well with observations of homogeneous freezing temperature increasing with increased drop size. Changing the drop size can impact the freezing temperature from around 1 °C to 5 °C (O and Wood, 2016; Tobo, 2016).

There is often a discrepancy between cold-stage and chamber ice nucleation efficiency results, with cold-stage methods underestimating ice nucleation efficiency. The cause of this discrepancy is thought to be a reduction of particle surface area in the suspension during the experiment due to coagulation (Emersic et al., 2015; Hiranuma et al., 2015). While coagulation can occur in suspensions of pure mineral and mineral dust powders, its impact on the resulting $n_s(T)$ values varies depending on the substance being studied. For example, by calculating the $n_s(T)$ values for suspensions of a range of weight percents and checking for self-consistency, Whale et al. (2015) determined that coagulation does not have a substantial impact on suspensions of NX-illite

or K-feldspar. Tests should be performed on new substances to determine whether or not coagulation will have a substantial impact on the results.

Chapter 3

Results

Once the freezing temperatures were collected for all the drops, the fraction frozen as a function of temperature, $f_i(T)$, was calculated for each run using Eq. (1.2). Figure 3.1 shows the fraction frozen vs temperature data for all the runs, and Fig. 3.2 shows only the glacial flour runs. In each graph the $f_i(T) = 0.5$ line was also plotted. The fifty percent fraction frozen (T_{50}) value is important because it is often chosen as the reference value when comparing results because it is less prone to variability than initial freezing temperature values (Zolles et al., 2015). While T_{50} is better than using initial freezing temperature when comparing results, there is still some variation in T_{50} between experiments due to differences in drop size and experiment methods. Statistical values are also presented using a box-and-whiskers plot of the freezing temperature data from the NX-illite and glacial flour runs (Fig. 3.3).

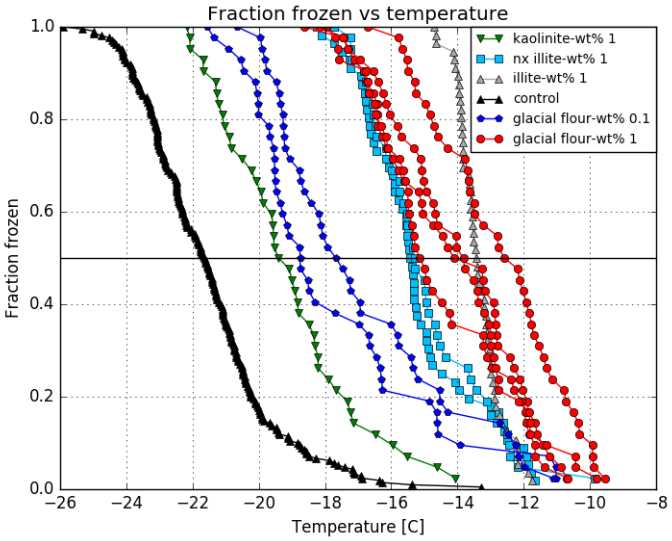

Figure 3.1: Plot of the fraction frozen as a function of temperature for all the runs. The horizontal line indicates the point where 50% of the drops are frozen.

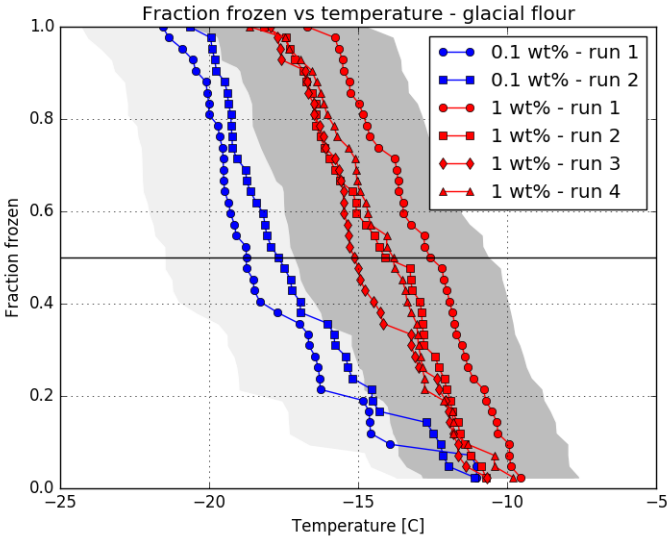

Figure 3.2: Plot of the fraction frozen as a function of temperature for only the glacial flour runs. The horizontal line indicates the point where 50% of the drops are frozen. The shaded areas represent one standard deviation in the temperature data. The lighter grey corresponds to the 0.1% glacial flour runs, and the darker grey the 1% glacial flour runs.

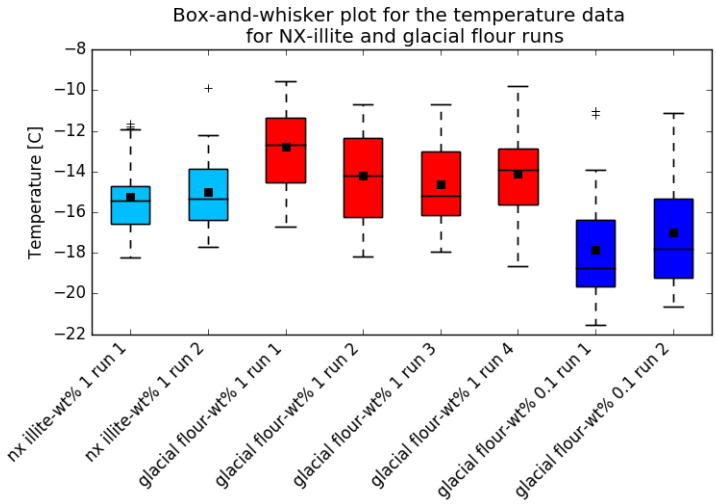

Figure 3.3: A box-and-whiskers plot of the freezing temperature data from the NX-illite and glacial flour runs. The box represents the interquartile range (IQR) of the data and the upper and lower whiskers represent $Q_3 + 1.5(IQR)$ and $Q_1 - 1.5(IQR)$ respectively. Any data points outside of these values are plotted as outlier points. The horizontal line in the boxes represents the median and the point inside the boxes represents the mean.

3.1 Control

To get a baseline and determine a threshold value for homogeneous nucleation, two runs were performed using pure water. These runs resulted in a homogeneous freezing temperature range of $-13.3\,^{\circ}\mathrm{C}$ to $-25.9\,^{\circ}\mathrm{C}$ and $T_{50} = -21.6\,^{\circ}\mathrm{C}$.

3.2 Reference Materials

Tests using NX-illite, illite, and kaolinite were performed to compare the experiment method with previous studies and to provide a same-method comparison for the glacial flour runs. Kaolinite was the least efficient INP with a freezing temperature range between $-14.1\,^{\circ}\mathrm{C}$ and $-22.2\,^{\circ}\mathrm{C}$ and $T_{50} = -19.4\,^{\circ}\mathrm{C}$. NX-illite gave a freezing temperature range between $-9.9\,^{\circ}\mathrm{C}$ and $-18.2\,^{\circ}\mathrm{C}$ and the T_{50} was $-15.4\,^{\circ}\mathrm{C}$ and $-15.3\,^{\circ}\mathrm{C}$ for runs 1 and 2 respectively. Illite gave some of the highest freezing temperatures

with a range between $-11.75\,^{\circ}\mathrm{C}$ and $-14.7\,^{\circ}\mathrm{C}$ and $T_{50} = -13.4\,^{\circ}\mathrm{C}$. These results all agree well with Whale et al. (2015) and qualitatively agree well with other studies (e.g. Murray et al., 2012; Atkinson et al., 2013). For the NX-illite, $n_s(T)$ was also calculated. The resulting $n_s(T)$ values ranged from 1.8×10^{-2} cm^{-2} to 4.0×10^{0} cm^{-2}.

3.2.1 Repeatability Validation

Two runs were performed using NX-illite to verify that the experiment method could provide repeatable results. As Fig. 3.1 shows, the two runs produced nearly identical results, and so it can be assumed with confidence that any variability between runs is due to variability in the sample not in the experiment method.

3.3 Glacial Flour

Glacial flour was the sample of interest for this study, so four runs were performed using 1 wt% suspensions and two were performed using 0.1 wt%.

3.3.1 Weight Percent 1

The 1 wt% glacial flour suspensions produced freezing temperature ranges between $-9.6\,^{\circ}\mathrm{C}$ and $-18.6\,^{\circ}\mathrm{C}$. Unlike the runs with NX-illite, there was a spread of values between the different glacial flour runs. The T_{50} value ranged from $-12.6\,^{\circ}\mathrm{C}$ to $-15.1\,^{\circ}\mathrm{C}$. Runs 2 and 4 agreed reasonably well, and run 3 agreed with those runs at the high and low ends of the temperature range but deviated in the middle. Run 1 was uniformly warmer than the other runs but had a similar trend to runs 2 and 4. This spread of values is expected due to the fact that glacial flour is a natural dust with a complex and varying composition. The $n_s(T)$ values ranged from 3.0×10^{-3} cm^{-2} to 5.0×10^{-1} cm^{-2}.

3.3.2 Weight Percent 0.1

The range of freezing temperatures for the 0.1 wt% suspensions was from $-11.0\,^{\circ}$C to $-21.6\,^{\circ}$C. Again there was a spread of values between the runs with the T_{50} value ranging from $-17.7\,^{\circ}$C to $-18.8\,^{\circ}$C. The majority of the drops in this set froze at lower temperatures than those of the 1 wt% set, with only a few initial freezing points overlapping with the 1 wt% set. This trend of freezing temperature decreasing with decreasing weight percent is as expected because when the weight percent is decreased for a set volume the number of particles in that volume will also decrease. Ice nucleation scales with surface area, so by decreasing the number of particles, and therefore the available surface area, the ice nucleation temperature is also decreased. The $n_s(T)$ values ranged from 3.1×10^{-2} cm^{-2} to 4.1×10^{0} cm^{-2}.

3.4 Comparison of $n_s(T)$ Values

The $n_s(T)$ data for NX-illite and glacial flour are presented in Fig. 3.4 and the glacial flour $n_s(T)$ data with error bars are presented in Fig. 3.5. As this data shows, glacial flour has an ice nucleation efficiency similar to that of NX-illite. By performing runs using multiple weight percents and checking for self-consistency it is possible to estimate if coagulation has an impact on the results (Whale et al., 2015). The $n_s(T)$ values for the glacial flour runs are self-consistent within the errors, so coagulation can be assumed to not have a substantial impact.

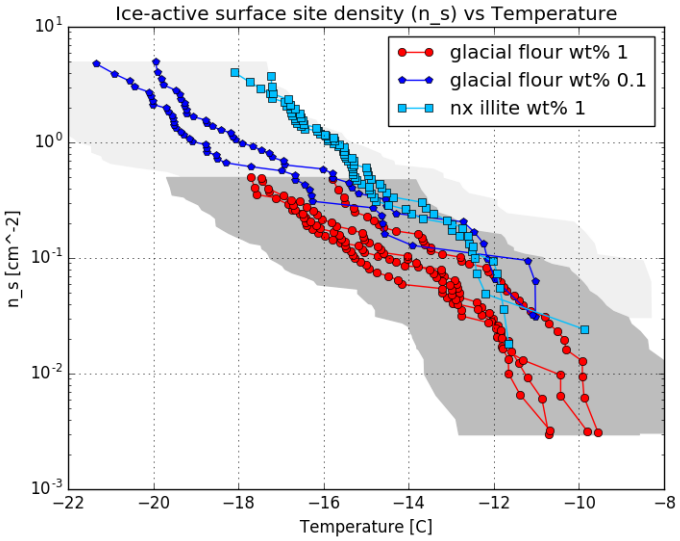

Figure 3.4: Plot of $n_s(T)$ for the NX-illite and glacial flour runs. The shaded areas represent one standard deviation in the temperature data. The lighter grey corresponds to the 0.1% glacial flour runs, and the darker grey the 1% glacial flour runs.

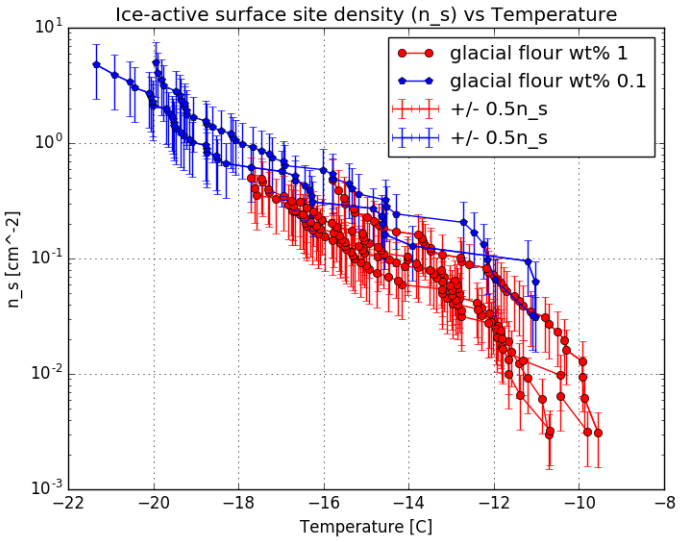

Figure 3.5: Plot of $n_s(T)$ for the glacial flour runs. The error bars represent $\pm$ 0.5 of the $n_s(T)$ value. The value for the error bars was determined by error propagation calculations.

Due to differences in experiment methods, it is challenging to compare the results from this study to those of previous studies. The best comparison can be made with Whale et al. (2015) which shows similar NX-illite results to this study with $n_s(T)$ values ranging from 10^1 cm^{-2} to to 10^{-2} cm^{-2}. The temperature range of that study is shifted a few degrees lower due to differences in cold stage setup and drop size, but even so the values from this study can be taken to be consistent with theirs.

Qualitative comparisons can also be used with some studies to evaluate where glacial flour ranks among pure minerals and other dusts. The $n_s(T)$ values of the glacial flour and NX-illite were close together, so NX-illite data can be used to get an idea of where the glacial flour stands. Murray et al. (2012) present a compilation of $n_s(T)$ data from multiple sources which includes both NX-illite and natural dusts. As can be seen in Fig. 12 of that paper, NX-illite, and by extension the glacial flour used in this study, has lower $n_s(T)$ values than the natural desert dusts. Atkinson et al. (2013) presented $n_s(T)$ values for some pure minerals and comparison of Fig. 1b of that paper with NX-illite data from this and previous studies suggests that NX-illite and glacial flour give $n_s(T)$ values that are lower than quartz and feldspars but higher than minerals such as montmorillonite, kaolinite, and calcite. This comparison suggests that the glacial flour sample studied here is not a highly efficient INP. Rather it falls around mid-range of the other dusts and pure minerals that have been studied.

Chapter 4

Discussion

4.1 Glacial Flour Constituent Contributions Based on Weight Percent and Surface Area Percent

Using the X-ray diffraction data, the contribution of each mineral constituent was evaluated based on weight percent. When ranked by weight percent, quartz would seem to be the most important constituent and albite the second most important with the others having a much smaller impact (Table 2.1). Because $n_s(T)$ is inversely proportional to surface area, the contribution of each constituent to the total surface area was evaluated by calculating the surface area percent of each constituent.

The surface area percent (SA%) was calculated using Eq. (3.1)

$$SA\%_i = \frac{(wt\%_i)(SSA_i)}{\Sigma((wt\%_i)(SSA_i))} \tag{4.1}$$

where SSA is the specific surface area of the constituent and the i subscript represents the individual constituents. The calculated SA% values and the estimates from literature for the SSA are given in Table 4.1. Evaluating the contribution of each constituent based on surface area percent gives a different result to the evaluation based on weight percent. Montmorillonite, which has the lowest weight percent, has the highest surface area percent and quartz has the second highest. Albite, while having the second highest weight percent, contributes less than half a percent of the total surface area. This surface area percent based ranking better explains the observed

$n_s(T)$ values than the ranking based on weight percent. Atkinson et al. (2013) performed a cold-stage experiment using montmorillonite, quartz, and Na/Ca-feldspar. By extrapolating the $n_s(T)$ data from Fig. 1b of that paper, the glacial flour data of this study would fall between montmorillonite and quartz. This result agrees well with surface area percent ranking, but not with the weight percent rating.

Table 4.1: Composition of glacial flour sorted by surface area percent. The specific surface area used in the surface area percent calculation and the source that specific surface area value are also listed.

Name	SA%	SSA [m^2g^{-1}]	SSA Source
Montmorillonite	48.8	640	(Cerato and Lutenegger, 2002)
Quartz	39.5	5.5	(Zolles et al., 2015)
Clinochlore	9.9	26	(Jones, 1981)
Muscovite	1.1	2.3	(Kini et al., 1968)
Protomangano-ferro-anthophyllite	0.5	1.21	(Chen and Brantley, 1998)
Albite	0.2	0.119	(Brantley and Mellott, 2000)

4.2 Glacial Flour Compared To Desert Dust

Most ice nucleation studies of natural dusts focus on desert dusts. However, there are differences between glacial flour and desert dust that make studying both important. The major difference is that the dusts come from different source regions, and, as a result, have different compositions. The composition of desert dust varies between studies due to different samples and analysis methods being used, but there are seven constituents that regularly appear. Schutz and Sebert (1987), Kandler et al. (2009), and Scheuvens and Kandler (2014) all report compositions for dust from the Sahara Desert, and, while none of the reported compositions are exactly the same, they all report the following seven constituents: quartz, K-feldspar, plagioclase, calcite, illite, kaolinite, and chlorite. Some other constituents that are sometimes reported in desert dust compositions include: montmorillonite, Na-feldspar, Ca-feldspar, and muscovite

(e.g. Schutz and Sebert, 1987; Murray et al., 2012; Scheuvens and Kandler, 2014). Of the seven minerals reported in all desert dust samples only two, quartz and chlorite, were found in the glacial flour sample used in this study. In the case of glacial flour from volcanic regions, plagioclase is the only mineral in common.

4.3 Comparison Of Dust Emission Sources

It is estimated that 1000 to 3000 Tg of mineral dust are emitted into the atmosphere each year (Thorsteinsson et al., 2011; Murray et al., 2012). The majority is thought to originate in arid tropical to mid-latitude regions, particularly North Africa and Asia. These two regions are the focus of most dust emission studies, but there are other sources that are important to consider as well. High latitude dust sources, in particular, have often been overlooked, but in the last few years studies of dust emissions in Iceland and Alaska have suggested that high latitude dust emissions are more substantial than previously assumed.

Deserts are undoubtedly a major source of dust due to their lack of precipitation and vegetation allowing the soil to easily be lofted into the atmosphere. Deserts also cover an extensive area with around 30% of the earth's land surface being classified as such (Schutz and Sebert, 1987). Individual glacial flour sources are much smaller, typically on the order of a few hundred to a few thousand km^2, but the number of potential sources is substantial. There are more than 100,000 glaciers globally and around 10% of the earth's land surface is covered in glacial ice (NSIDC, 2017). All glaciers will produce glacial flour, but the exact amount that will be lofted into the atmosphere depends on a number of local characteristics such as glacial outwash paths, vegetation and snow cover, precipitation patterns, and wind profiles to name a few. The remoteness of many of these high latitude locations means that few measurements of these characteristics or the dust emissions associated with them have been collected.

Bullard et al. (2016) estimate that high latitude dust sources could contribute 80 to 100 Tg per year to global mineral dust emissions. This estimate was determined based off of published emission estimates for only four regions (South America, Patagonia,

Iceland, and Alaska), which means the total emission could potentially be even higher if other high latitude source regions are considered. High latitude dust emission amounts are also expected to rise as global warming leads to a retreat of glaciers (Thorsteinsson et al., 2011; Prospero et al., 2012; Bullard et al., 2016).

Estimates for annual dust emissions for high latitude dust as well as five tropical to mid-latitude regions are given in Table 4.2. For emission ranges, the median value was used in the percentage calculation. As expected, North Africa and East Asia have the highest dust emission values. High latitude dust emission is on par with dust emission from Australia, supporting the idea that such dust could be an important source of INP.

Table 4.2: Dust emission rates for six regions. Total global dust emission assumed to be 2000 Tg yr^{-1}. Median value of emission ranges was used when calculating the percentages. The emission values for North Africa and East Asia are from Scheuvens and Kandler (2014), and all other values are from Bullard et al. (2016). The value for North America excludes emissions from Alaska and Canada.

Region	Dust Emission [Tg yr^{-1}]	Percent of Total Emission
North Africa	700	35
East Asia	250	12.5
Australia	37-148	4.6
High Latitude	80-100	4.5
South Africa	63	3.2
North America	2-53	1.4

4.4 Potential For Pre-activation Of Glacial Flour Particles

Another process that could have an impact on the ice nucleation efficiency of mineral and dust particles is pre-activation. Pre-activation is the process in which an INP gains an enhanced ice nucleation efficiency from either remnant ice crystals from previous

ice nucleation events or the homogeneous freezing of supercooled water from pore condensation (Roberts and Hallett, 1968; Higuchi and Wushiki, 1970; Wagner et al., 2016).

Pore condensation, also termed capillary condensation in some literature, describes condensation that forms within small pores or capillaries. The concave liquid-vapor interface that forms in the capillary leads to a reduction of the free energy barrier by lowering the vapor pressure over the interface. The lower vapor pressure leads to water condensing in the capillary below saturation (Christenson, 2013).This capillary contained liquid can then freeze homogeneously, which will enhance the ice nucleation efficiency of the INP it is contained in. Similarly, if the INP was previously involved in ice nucleation, pockets of ice crystals can remain in pores even in environments that are below ice saturation. These ice crystals can then enhance ice nucleation when the INP returns to a saturated environment (Wagner et al., 2016).

Pre-activation has been observed in multiple materials and studies (e.g. Roberts and Hallett, 1968; Higuchi and Wushiki, 1970; Wagner et al., 2016). Roberts and Hallett (1968) studied the ice nucleation and pre-activation characteristics of multiple mineral and dust samples and found that many were susceptible to pre-activation. Three of the samples that were tested were collected from glacier outwash streams in Washington, Norway, and Switzerland. For all three samples, pre-activation increased the threshold ice nucleation temperature by between $-2.5\,^{\circ}\mathrm{C}$ to $-9.5\,^{\circ}\mathrm{C}$. Higuchi and Wushiki (1970) made in-situ measurements of pre-activated INPs at Barrow, Alaska, and found that pre-activated INPs could be found near the surface in high latitude regions.

Due to the sample preparation and experimental method used in this study, the impact of pre-activation on the glacial flour sample could not be evaluated. It appears likely that the glacial flour used in this study would be susceptible to pre-activation, but further studies would need to be performed to know exactly how much the ice nucleation efficiency would be impacted.

Chapter 5

Conclusions

Immersion freezing is a dominant ice nucleation mode, so understanding what materials can act as INPs in this mode and how efficient they are is important for understanding and representing cloud and precipitation processes. In this study, a cold-stage freezer method was used to evaluate the ice nucleation efficiency of four materials: glacial flour, NX-illite, illite, and kaolinite. The freezing temperatures of NX-illite, illite, and kaolinite were found to agree with literature values. No previous studies have been performed using glacial flour. XDR analysis indicated that the glacial flour was composed of mostly quartz and albite, 70.246 wt% and 16.470 wt% respectively (Table 2.1). Other minerals that were present in smaller fractions included: muscovite (4.617 wt%), protomangano-ferro-anthophyllite (4.195 wt%), clinochlore (3.708 wt%), and montmorillonite (0.746 wt%). The BET surface area was found to be 4.7160 ± 0.0345 m^2g^{-1}. The glacial flour sample produced immersion freezing temperatures between $-9.6\,^{\circ}C$ and $-21.6\,^{\circ}C$, which corresponds to $n_s(T)$ values between 3.0×10^{-3} cm^{-2} and 4.1×10^{0} cm^{-2}. These values are similar to those found for NX-illite, indicating that the glacial flour sample falls around mid-range of the mineral and dust samples that have been previously studied.

The dominance of different minerals in a dust is often evaluated using the weight percent. However, the evaluation of the glacial flour constituents suggests that surface area percent may be a better representative of ice nucleation efficiency. The weight percent evaluation (Table 2.1) ranked quartz and albite as the most dominant minerals,

but the surface area evaluation (Table 4.1) ranked montmorillonite (48.8 SA%) and quartz (39.5 SA%) as the most dominant, which corresponds well to the $n_s(T)$ values of the glacial flour falling between those of montmorillonite and quartz.

Most dust studies have focused on arid tropical to mid-latitude dust sources with high latitude sources being given little attention. While the strongest individual sources are found within tropical to mid-latitude regions, the total contribution of high latitude sources is not negligible. One estimate of high latitude dust emissions is 80 to 100 Tg yr^{-1}, which puts it on par with dust emission from Australia (Table 4.2). This emission estimate could increase as retreating glaciers expand dust deposits, making glacial flour, and other forms of high latitude dust, an even greater source of INPs.

A quantitative study of the impact of pre-activation of glacial flour was not studied here, but literature results suggest that pre-activation could potentially increase the freezing temperature of glacial flour suspensions by as much as 10 °C. Further studies would need to be conducted to determine the exact impact of pre-activation on the glacial flour sample used here.

Bibliography

Atkinson, J. D., Murry, B. J., Woodhouse, M. T., Whale, T. F., Baustian, K. J., Carslaw, K. S., Dobbie, S., O'Sullivan, D., and Malkin, T. L.: The importance of feldspar for ice nucleation by mineral dust in mixed-phase clouds, Nature, 498, 355–358, doi:10.1038/nature12278, 2013.

Augustin-Bauditz, S., Wex, H., Kanter, S., Ebert, M., Niedermeier, D., Stolz, F., Prager, A., and Stratmann, F.: The immersion mode ice nucleation behavior of mineral dusts: A comparison of different pure and surface modified dusts, Geophys. Res. Lett., 41, 73757382, doi:10.1002/2014GL061317, 2014.

Brantley, S. L. and Mellott, N. P.: Surface area and porosity of primary silicate minerals, American Mineralogist, 85, 1767–1783, 2000.

Broadley, S. L., Murray, B. J., Herbert, R. J., Atkinson, J. D., Dobbie, S., Malkin, T. L., Condliffe, E., and Neve, L.: Immersion mode heterogeneous ice nucleation by an illite rich powder representative of atmospheric mineral dust, Atmos. Chem. Phys., 12, 287–307, doi:10.5194/acp-12-287-2012, 2012.

Brucker-AXS: TOPAS V4: General profile and structure analysis software for powder diffraction data, User guide, 2008.

Bullard, J. E., Baddock, M., Bradwell, T., Crusius, J., Darlington, E., Gaiero, D., Gasso, S., Gisladottir, G., Hodgkins, R., McCulloch, R., McKenna-Neuman, C., Mockford, T., Stewart, H., and Thorsteinsson, T.: High-latitude dust in the Earth system, Reviews of Geophysics, 54, 447–485, doi:10.1002/2016RG000518, 2016.

Cerato, A. B. and Lutenegger, A. J.: Determination of surface area of fine-grained soils by the ethylene glycol monoethyl ether (EGME) method, Geotechnical Testing Journal, 25(3), 315–321, 2002.

Chen, Y. and Brantley, S. L.: Diopside and anthophyllite dissolution at 25 °C and 90 °C and acid pH, Chemical Geology, 147, 233–248, 1998.

Christenson, H. K.: Two-step crystal nucleation via capillary condensation, CrystEngComm, 15, 2030–2039, doi:10.1039/c3ce26887j, 2013.

Connolly, P. J., Mohler, O., Field, P. R., Saathoff, H., Burgess, R., Choularton, T., and Gallagher, M.: Studies of heterogenous freezing by three different desert dust samples, Atmos. Chem. Phys., 9, 2805–2824, doi:10.5194/acp-9-2805-20097, 2009.

Dagsson-Waldhauserova, P., Arnalds, O., Olafsson, H., Skrabalova, L., Sigurdardottir, G. M., Branis, M., Hladil, J., Skala, R., Navratil, T., Chadimova, L., von Lowis of Menar, S., Thorsteinsson, T., Carlsen, H. K., and Jonsdottir, I.: Physical properties of suspended dust during moist and low wind conditions in Iceland, Icelandic Agricultural Sciences, 27, 25–39, 2014.

Emersic, C., Connolly, P. J., Boult, S., Campana, M., and Li, Z.: Investigating the discrepancy between wet-suspension- and dry-dispersion-derived ice nucleation efficiency of mineral particles, Atmos. Chem. Phys., 15, 11 311–11 326, doi:10.5194/acp-15-11311-2015, 2015.

Ervens, B. and Feingold, G.: Sensitivities of immersion freezing: Reconciling classical nucleation theory and deterministic expressions, Geophysical Research Letters, 40, 3320–3324, doi:10.1002/grl.50580, 2013.

Froitzheim, N.: Origin of the Monte Rosa nappe in the Pennine Alps - a new working hypothesis, GSA Bulletin, 113(5), 2001.

Groot Zwaaftink, C. D., Arnalds, O., Dagsson-Waldhauserova, P., Eckhardt, S., Prospero, J. M., and Stohl, A.: Temporal and spatial variability of Icelandic dust emission and atmospheric transport, Atmospheric Chemistry and Physics Discussions, 2017, 1–23, doi:10.5194/acp-2017-290, 2017.

Higuchi, K. and Wushiki, H.: Observations of pre-activated ice nuclei in the atmosphere at subzero temperature, Journal of the Meteorological Society of Japan, 48(3), 250–254, 1970.

Hiranuma, N., Augustin-Bauditz, S., Bingemer, H., Budke, C., Curtius, J., Danielczok, A., Diehl, K., Dreischmeier, K., Ebert, M., Frank, F., Hoffmann, N., Kandler, K., Kiselev, A., Koop, T., Leisner, T., Möhler, O., Nillius, B., Peckhaus, A., Rose, D., Weinbruch, S., Wex, H., Boose, Y., DeMott, P. J., Hader, J. D., Hill, T. C. J., Kanji, Z. A., Kulkarni, G., Levin, E. J. T., McCluskey, C. S., Murakami, M., Murray, B. J., Niedermeier, D., Petters, M. D., O'Sullivan, D., Saito, A., Schill, G. P., Tajiri, T., Tolbert, M. A., Welti, A., Whale, T. F., Wright, T. P., and Yamashita, K.: A comprehensive laboratory study on the immersion freezing behavior of illite NX particles: a comparison of 17 ice nucleation measurement techniques, Atmos. Chem. Phys., 15, 2489–2518, doi:10.5194/acp-15-2489-2015, 2015.

Jones, A. A.: Charges on the surfaces of two chlorites, Clay Minerals, 16, 347–359, 1981.

Kandler, K., Schutz, L., Deutscher, C., Ebert, M., Hofmann, H., Jackel, S., Jaenicke, R., Knippertz, P., Lieke, K., Massling, A., Petzold, A., Schladitz, A., Weinzierl, B., Wiedensohler, A., Zorn, S., and Weinbruch, S.: Size distribution, mass concentration, chemical and mineralogical composition and derived optical parameters of the boundary layer aerosol at Tinfou, Morocco, during SAMUM 2006, Tellus, 61B, 32–50, doi:10.1111/j/1600-0889.2008.00385.x, 2009.

Kini, K. A., Manser, R. M., and Joy, A. S.: The surface area of silicate minerals by the BET method using the absorption of xenon at −78 °C, Journal of Physical Chemistry, 72(6), 2127–2129, 1968.

Marcus, Y.: Effect of ions on the structure of water: structure making and breaking, Chemical Reviews, 109(3), 1346–1370, 2009.

Murray, B. J., O'Sullivan, D., Atkinson, J. D., and Webb, M. E.: Ice nucleation by particles immersed in supercooled cloud droplets, Chem. Soc. Rev., 41, 6519–6554, doi:10.1039/c2cs35200a, 2012.

NSIDC: Facts About Glaciers, http://nsidc.org/cryosphere/glaciers/quickfacts.html, last access: 2 August 2017, 2017.

O, K.-T. and Wood, R.: Exploring an approximation for the homogeneous freezing temperature of water droplets, Atmos. Chem. Phys., 16, 7239–7249, doi: 10.5194/acp-16-7239-2016, 2016.

Prospero, J. M., Ginoux, P., Torres, O., Nicholson, S. E., and Gill, T. E.: Environmental characterization of global sources of atmosphereic soil dust identified with the Nimbus 7 Total Ozone Mapping Spectrometer (TOMS) absorbing aerosol product, Rev. Geophys., 40(1), doi:10.1029/2000RG000095, 2002.

Prospero, J. M., Bullard, J., and Hodgkins, R.: High-latitude dust over the North Atlantic: inputs from icelandic proglacial dust storms, Science, 335, 1078–1082, doi:10.1126/science.1217447, 2012.

Rampe, E. B., Horgan, B., Scudder, N., Smith, R. J., and Rutledge, A. M.: Mineralogy of rock flour in glaciated volcanic terrains: an analog for a cold and icy early mars, Lunar and Planetary Science, 48, 2017.

Roberts, P. and Hallett, J.: A laboratory study of the ice nucleating properties of some mineral particulates, Quarterly Journal of the Royal Meteorological Society, 94, 25–34, 1968.

Rogers, R. R. and Yau, M. K.: A short course in cloud physics, Butterworth Heinemann, Oxford, 3 edn., 1996.

Scheuvens, D. and Kandler, K.: On composition, morphology, and size distribution of airborne mineral dust, in: Mineral dust: a key player in the Earth system, edited

by Knippertz, P. and Stuut, J.-B. W., pp. 15–49, Springer Netherlands, Dordrecht, 2014.

Schutz, L. and Sebert, M.: Mineral aerosols and source identification, J. Aerosol Sci., 18, 1–10, 1987.

Thorsteinsson, T., Gisladottir, G., Bullard, J., and McTainsh, G.: Dust storm contributions to airborne particulate matter in Reykjavik, Iceland, Atmospheric Environment, 45, 5924–5933, doi:10.1016/j.atmosenv.2011.05.023, 2011.

Tobo, Y.: An improved approach for measuring immersion freezing in large droplets over a wide temperature range, Sci. Rep., 6, doi:10.1038/srep32930, 2016.

Vali, G., DeMott, P. J., Mohler, O., and Whale, T. F.: Technical note: a proposal for ice nucleation terminology, Atmos. Chem. Phys., 15, 10 263–10 270, doi:10.5194/acp-15-10263-2015, 2015.

Wagner, R., Kiselev, A., Mohler, O., Saathoff, H., and Steinke, I.: Pre-activation of ice-nucleating particles by the pore condensation and freezing mechanism, Atmos. Chem. Phys., 16, 2025–2042, doi:10.5194/acp-16-2025-2016, 2016.

Whale, T. F., Murray, B. J., O'Sullivan, D., Wilson, T. W., Umo, N. S., Baustian, K. J., Atkinson, J. D., Workneh, D. A., and Morris, G. J.: A technique for quantifying heterogeneous ice nucleation in microlitre supercooled water drops, Atmos. Meas. Tech., 8, 2437–2447, doi:10.5194/amt-8-2437-2015, 2015.

Zolles, T., Burkart, J., Hausler, T., Pummer, B., Hitzenberger, R., and Grothe, H.: Identification of ice nucleation active sites on feldspar dust particles, J. Phys. Chem. A, 119, 2692–2700, doi:10.1021/jp509839x, 2015.

Appendix A

XDR Diffractogram for Glacial Flour Sample

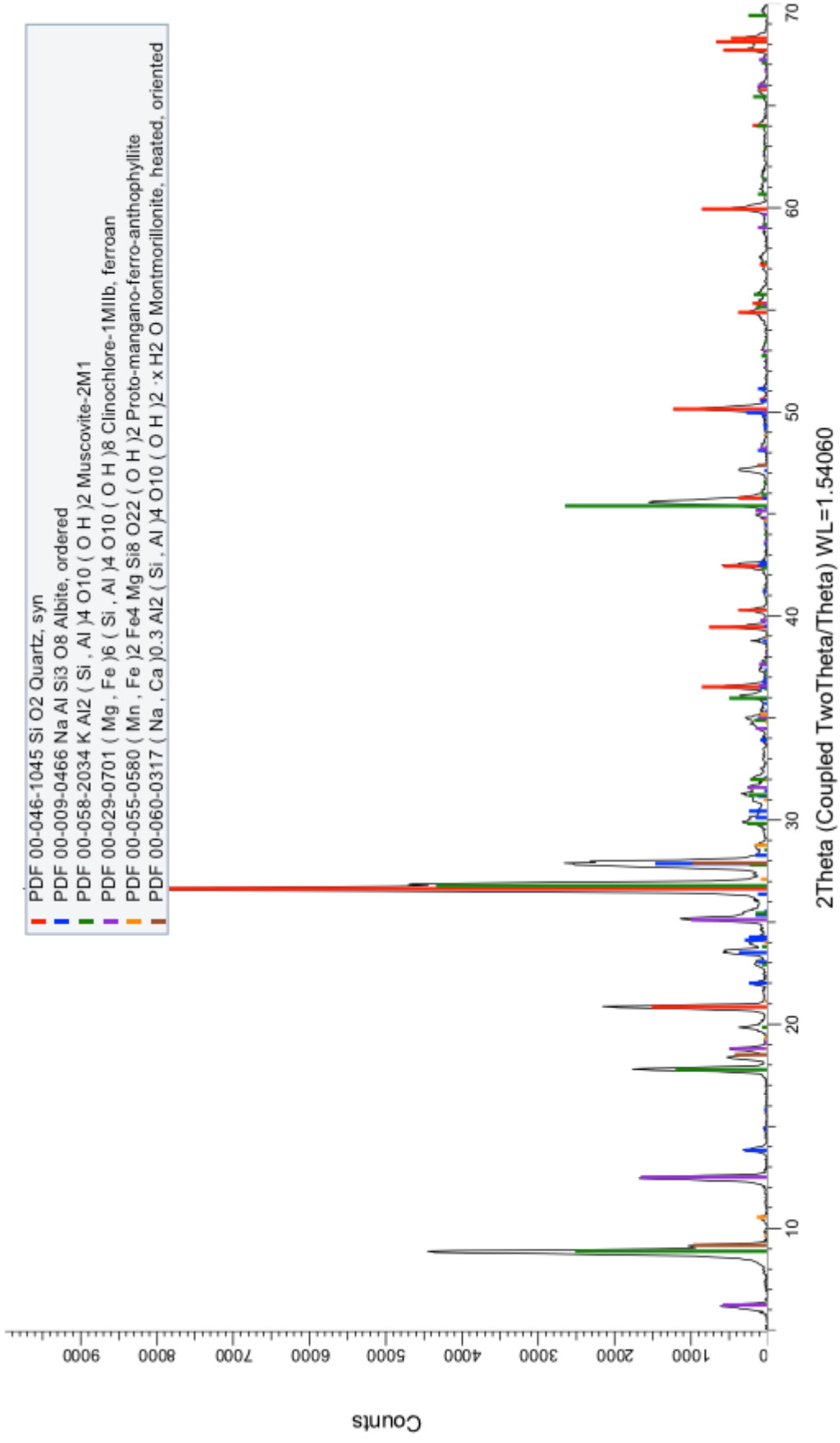

Figure A.1: XDR diffractogram for the glacial flour sample.

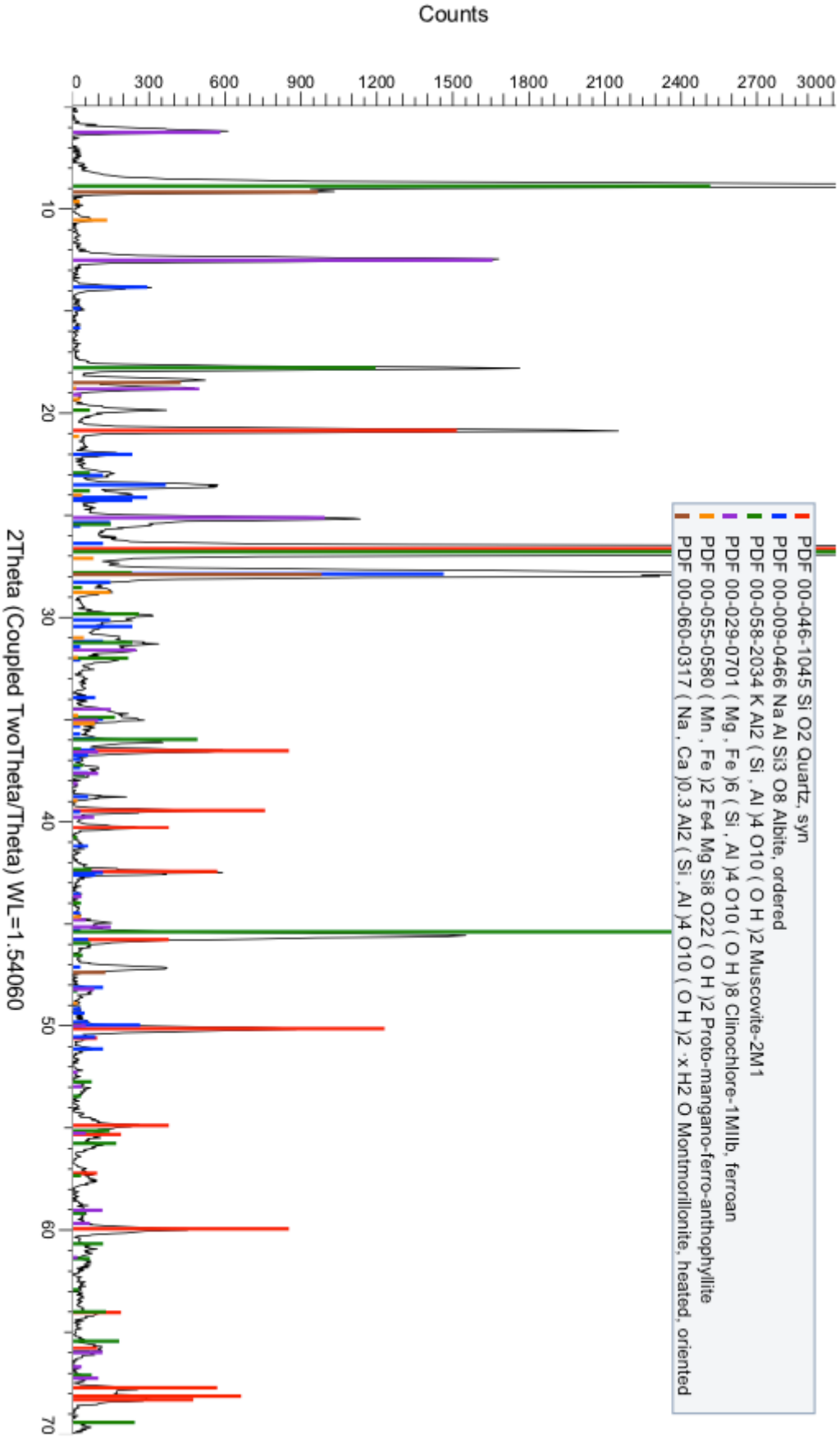

Figure A.2: Zoomed in plot of the XDR diffractogram to show the smaller scale details